ERJ Express. Published on October 25, 2012 as doi: 10.1183/09031936.00015612

CELL CYCLE-DEPENDENCE OF ACE-2 EXPLAINS DOWNREGULATION IN IDIOPATHIC PULMONARY FIBROSIS

Bruce D. Uhal[1], MyTrang Dang[1], Vinh Dang[1], Roger Llatos[2], Esteban Cano[3], Amal Abdul-Hafez[4], Jonathan Markey[1], Christopher C. Piasecki[1] and Maria Molina-Molina[2]

[1]Department of Physiology, Michigan State University, East Lansing, Michigan, 48824; [2]Unidad de Intersticio Pulmonar, Servicio de Neumologia, Hospital Universitario de Bellvitge, IDIBELL, España; [3]Instituto del Tórax, Hospital Clínic de Barcelona, c/Villaroel 170, 08023, España; [4]College of Pharmacy, Misr International University, Cairo, Egypt

Running Head: Downregulation of ACE-2 by cell proliferation

Address all correspondence and reprint requests to:

Bruce D. Uhal, Ph.D.

Department of Physiology

Michigan State University

3197 Biomedical and Physical Sciences Building

East Lansing, MI 48824

Phone: (517)355-6475 x1144

Fax: (517)355-5125

Email: uhal@msu.edu

ABSTRACT

Alveolar epithelial type II cells, a major source of angiotensin converting enzyme-2 in the adult lung, are normally quiescent but actively proliferate in lung fibrosis and downregulate this protective enzyme. It was therefore hypothesized that angiotensin converting enzyme-2 expression might be related to cell cycle progression. To test this hypothesis, angiotensin converting enzyme-2 mRNA, protein and enzymatic were examined in fibrotic human lung and in the AEC cells lines A549 and MLE-12 studied at postconfluent (quiescent) versus subconfluent (proliferating) densities. Angiotensin converting enzyme-2 mRNA, immunoreactive protein and enzymatic activity were all high in quiescent cells, but were severely downregulated or absent in actively proliferating cells. Upregulation of enzyme in cells that were progressing to quiescence was completely inhibited by the transcription blocker actinomycin D or by SP600125, an inhibitor of c-Jun N-Terminal Kinase. In lung biopsy specimens obtained from patients with Idiopathic Pulmonary Fibrosis, immunoreactive enzyme was absent in alveolar epithelia that were positive for proliferation markers, but was robustly expressed in alveolar epithelia devoid of proliferation markers. These data explain the loss of angiotensin converting enzyme-2 in lung fibrosis and demonstrate cell cycle-dependent regulation of this protective enzyme by a JNK-mediated transcriptional mechanism.

Key Words: alveolar epithelium; lung fibrogenesis; hyperplastic epithelium; Interstitial Lung Disease; angiotensin1-7/mas axis

INTRODUCTION

A variety of investigations support the contention that a local tissue angiotensin (ANG) system is critical in the pathogenesis of pulmonary fibrosis in both animal models (1,2) and in Idiopathic Pulmonary Fibrosis (3,4), the most frequent and insidious interstitial lung disease (ILD) encountered by pulmonary physicians. Several lines of evidence point to a critical role for ANGII in the signaling of cellular and molecular events believed to be critical in the pathogenesis of lung fibrosis, including alveolar epithelial cell (AEC) apoptosis (5), fibroblast proliferation and migration (6,7) and collagen synthesis (8).

The induction of apoptosis in cultured AECs in response to a variety of proapoptotic and profibrotic stimuli (9,10,11,12) has been shown to both activate and require the synthesis of angiotensinogen (AGT) and the processed peptide ANGII, the effector peptide of this system. ANGII is both motogenic (7) and mitogenic (6) for human lung fibroblasts, and increases collagen synthesis through a mechanism that is mediated by autocrine transactivation of transforming growth factor-beta 1 (TGF-β1) in the fibroblast itself (8). TGF-β1 transactivation in turn stimulates procollagen synthesis and the myofibroblast transition (13,14), in addition to activating AGT expression in an apparent autocrine loop (13). Reductions of lung fibrogenesis by ANG receptor AT1 blockers in mice or rats (1,15) or AT1 receptor deletion in mice (1) support the contention that the mechanisms just discussed are active *in vivo* as well as the *in vitro* systems in which they were first identified.

Evidence from this laboratory supports an important role in lung fibrosis for the counterregulatory axis composed of angiotensin converting enzyme-2 (ACE-2), its product ANG1-7 and the ANG1-7 receptor *mas* (5). In the bleomycin model of lung fibrosis in mice or rats, ACE-2 was shown to be protective though the use of siRNA knockdown or competitive

inhibition of ACE-2 with the peptide DX600, either of which exacerbated collagen deposition in response to bleomycin (4). Other authors have shown a similar protective role for ACE-2 in lung fibrosis induced by monocrotaline (16). On the other hand, administration of purified recombinant ACE-2 inhibited bleomycin-induced collagen deposition (4).

In a recent study of the regulation of apoptosis in cultured AECs, ACE-2 and its product ANG1-7 were found to protect against AEC death through the ability of ANG1-7 to reduce JNK phosphorylation, an event required for the signaling of AEC apoptosis in response to ANGII and other proapoptotic inducers (5). The inhibitory effect of ANG1-7 on AEC death was mediated by the ANG1-7 receptor *mas*. Those results, together with those showing inhibition of collagen deposition discussed in the preceding paragraph, demonstrate the antiapoptotic and antifibrotic roles of the ACE-2/ANG1-7/mas axis in experimental pulmonary fibrosis.

An important finding in the study by Li et al. (4) was the demonstration that the protective enzyme ACE-2 was downregulated in both experimental and human lung fibrosis. In human lung tissue obtained by biopsy from patients with Idiopathic Pulmonary Fibrosis (IPF), ACE-2 was reduced at the level of mRNA, immunoreactive protein and enzymatic activity, all of which were reduced to a similar severe degree (ibid). Likewise, ACE-2 protein, enzymatic activity and mRNA were also reduced in bleomycin-induced mouse and rat models of IPF, but no reduction was seen in ACE-2 mRNA in cultured AECs exposed to bleomycin in vitro. For this reason, we sought to find a mechanism that could explain the loss of ACE-2 mRNA, protein and activity in fibrotic human lungs that were never exposed to bleomyin or other xenobiotic inducers of apoptosis.

For many years the alveolar epithelium of the fibrotic human lung has been described as the “hyperplastic” or “cuboidal” epithelium, based on the observation of predominantly type II

pneumocytes that are proliferating in response to ongoing epithelial injury (17,18). In contrast, the alveolar epithelium of normal lung is essentially quiescent, with little or no proliferating cells and numerous type I cells, the terminally differentiated progeny of type II cells (19). On this basis, it was hypothesized that the decrease in ACE-2 observed in fibrotic human lung (4) might be a consequence of cell cycle progression by type II pneumocytes. We report here the finding that ACE-2 mRNA, immunoreactive protein and enzymatic activity are all highly expressed in AECs that are quiescent, but are downregulated in AECs that have entered the cell cycle. We also report evidence that the upregulation of ACE-2 that accompanies the progression of AECs to quiescence is transcriptionally regulated by a mechanism mediated by Jun N-terminal Kinase.

MATERIALS AND METHODS

Materials. The fluorogenic peptide substrate MCA-YVADAPK(Dnp)-OH and purified human recombinant ACE-2 were obtained from R&D Systems, Minneapolis, MN. The peptide DX600 was synthesized by the Macromolecular Structure Facility (Department of Biochemistry, Michigan State University). Antibodies against ACE-2 and MNF-116 were obtained from Abcam, Cambridge, MA. Antibodies against PCNA and BrdU were purchased from BD Biosciences, San Diego, CA. Actinomycin D and SP600125 were purchased from Sigma-Aldrich, Saint Louis, MO. SB203580 was obtained from Cell Signaling, Danvers, MA and PD98059 was purchased from Invitrogen, Grand Island NY. Primers for RTPCR of ACE-2 were purchased from Santa Cruz Biotechnology Inc., Santa Cruz, CA. All other materials were of reagent grade.

Cell culture: The human lung adenocarcinoma cell line A549 was obtained from the American Type Cell Culture Collection and cultured in Ham's F12 medium supplemented with 10% fetal bovine serum (FBS). The mouse lung epithelial cell line MLE-12, a kind gift from the laboratory of Dr. Jeffrey Whitsett, University of Cincinatti, OH, was grown in complete HITES media supplemented with 5% FBS. All experiments were performed in the presence of serum regardless of the cell density. Subconfluent cells (SC) were harvested at 60-75% confluence, and postconfluent cells (PC) were harvested at five days postconfluence unless noted otherwise.

Human tissue samples and handling. Human lung tissue was obtained by video-assisted thoracoscopic lung surgery performed at Thorax Clínic Direction, University Hospital of Bellvitge. Fibrotic lung tissue was obtained from 14 patients with IPF; biopsies were obtained from more than one lung lobe. All patients had clinical, functional, radiological and histological features that fulfil the diagnostic criteria for IPF (20). Two different expert radiologists and

pathologists evaluated high-resolution tomography scan images and the histological pattern of the lung section respectively. Patients had neither antecedents of any occupational or environmental exposure nor any other known cause of ILD. The multidisciplinary committee of Interstitial Lung Diseases evaluated all cases. None of these IPF patients had received steroids or other immunosupressant therapy at the time of lung sample collection. Normal human lung tissue was obtained from 7 individuals undergoing surgical treatment for spontaneous pneumothorax with no history of pulmonary disease. No histopathological evidence of disease was found in these tissue samples. Written informed consent was obtained from the patients according to institutional guidelines, and the study was approved by the Ethics Committee of University Hospital of Bellvitge. All tissue was fixed in 10% neutral buffered formalin for 16 hours and embedded in paraffin. Sections were cut at 4.0 μm thickness and mounted on glass coverslips.

RNA isolation and reverse transcriptase polymerase chain reaction. Total RNA was extracted from human lung biopsies or frozen mouse lung with Trizol Reagent (Invitrogen) according to the manufacturer's instructions. First-strand cDNA was synthesized from 2 μg of total RNA with Superscript II reverse transcriptase (Invitrogen) and oligo (dT)12-18. Real-time RT-PCR was carried out with cDNA synthesized from 50 ng of total RNA, SYBR Green PCR core reagents (Applied Biosystems, Foster City, CA) according to the manufacturer's protocol, and 0.2 μM specific primers for human ACE-2: sense 5'-CATTGGAGCAAGTGTTGGATCTT-3', and antisense 5'-GAGCTA-ATGCATGCCA-TTCTCA-3') and β-actin (sense 5'-AGGCCAACCGCG-AGAAGATGACC-3' and antisense 5'-GAAGTCCAGGGCGACGTAGC-3'. For mouse ACE-2, the primers were: sense 5'-GGATACCTACCCTTCCTACATCAGC-3' and antisense 5'-CTACCC CACATATCACCAAGCA-3' and for mouse β-actin, sense 5'-TCCTGTGGCATCCAT-GAAACT-3' and antisense 5'-CTTCGTGAACGCCACGTG-CTA-3'.

The PCR thermal profile started with 10 minutes activation of Taq polymerase at 95ºC followed by 40 cycles of denaturation at 94ºC for 60s, annealing at 55ºC for 60s, and extension at 72ºC for 60s, ending with dissociation curve analysis to validate the specificity of the PCR products. Reactions were performed in a Mx3000P machine (Stratagene, La Jolla, CA) and threshold cycle (Ct) data were collected with MxPro-Mx3000P software version 3.0. The relative ACE-2 expression was normalized to β-actin and calculated with the comparative CT method of $2^{-\Delta\Delta CT}$. In all figures, the mean value for the ACE-2/β-actin ratio in the control group was set to 100%, and was expressed relative to the ACE-2/β-actin ratio for the treatment group.

Western blotting. Human or mouse lung epithelial cells were homogenized in ice-cold NP40-based lysis buffer, supplemented with protease inhibitor (Protease Inhibitor Cocktail P840, Sigma). Soluble protein extracts (20 μg) were loaded and run on 10% Tris-HCl polyacrylamide gels, separated by SDS-PAGE, in 10x Tris/Glycine/SDS buffer (BioRad). Gels were transferred to Immun-blot PVDF blotting membrane (Bio-Rad) in Towbin buffer. Blotting membrane was blocked by 5% nonfat dry milk in 0.1% Tween 20 in Tris-buffered saline. Western blot analysis of ACE-2 was performed with anti-ACE-2 polyclonal antibody (1:200 dilution; Santa Cruz Biotechnology). Bands were visualized by HRP-conjugated donkey anti-goat secondary antibody (1:2000 dilution; Santa Cruz Biotechnology) using the chemiluminescent substrate SuperSignal West Femto Maximum Sensitivity (Pierce, Rockford, IL). To ensure equal loading of proteins, membranes were stripped and then reprobed with an antibody against β-actin (Cell Signaling Technology).

ACE-2 enzyme assay. Protein was extracted from human biopsy samples or from mouse lung by homogenization in ice-cold Tris-HCl EDTA-free buffer, pH 6.5 (4). The enzymatic activity of ACE-2 proteins was measured immediately after homogenization by the cleavage of

fluorogenic substrate MCA-YVADAPK at 10uM, in 45 µl of lung tissue homogenate with Tris-HCl buffer pH 6.5 containing lisinopril (50ug/L) to block ACE activity (4,5). Reactions were performed in black microtiter plates at room temperature within a fluorescence microplate reader (FL600 Biotec Fluorescence Reader. BMG, Durham, NC, USA) during 30 minutes, using excitation and emission wavelengths of 310/20 and 420/50 nm.

Immunohistochemistry and Imunocytochemistry. Immunohistochemistry (IHC) for ACE-2, type II cell-specific cytokeratins and proliferating cell nuclear antigen (PCNA) was performed with anti-ACE-2 antibody (Abcam, 1:50 dilution), anticytokeratin antibody MNF-116 (Dako, 1:50 dilution) and an anti-PCNA monoclonal antibody (BD Biosciences, 1:100 dilution). Deparaffinized lung sections were blocked with a solution of 3% bovine serum albumin in PBS for 1 hour; the primary antibody was then applied overnight at 4°C in 3% bovine serum albumin/PBS. After washing in PBS, the antibody was detected with a biotin-conjugated secondary antibody and avidin-linked chromogen system. Chromogens were either diaminobenzidine (DAB, brown) or fast red (red). Immunohistochemistry was performed on ethanol-fixed AEC monolayers as described earlier (21) with anti-BrdU-FITC antibodies (BD Biosciences) or the same ACE-2 antibody used for western blotting.

Microscopy, Image Acquisition and Flow Cytometry. The prepared lung sections were photographed under transmitted or epifluorescent light on an Olympus BH2 epifluorescence microscope fitted with a SPOT Slider digital camera. Images of green fluorescence (anti-ACE-2 or BrdU) were acquired through a 520nm bandpass filter. Bivariate flow cytometric data for incorporated BrdU versus DNA distribution were performed as described earlier (22) on cells harvested by trypsinization. Flow cytometric data were acquired on an Accuri C6 laser flow cytometer (BD Accuri Cytometers, Ann Arbor, MI).

RESULTS

For the reasons described in the Introduction, the levels of ACE-2 protein, enzymatic activity and mRNA were examined in the human and mouse AEC cell lines A549 and MLE-12 under proliferating versus quiescent culture conditions, both in the presence of growth factors. Figure 1 Panels A and B show human alveolar epithelial A549 cells cultured under postconfluent and subconfluent, respectively, culture conditions, both in the presence of growth factors (i.e. both in the presence of serum). Panel C shows BrdU labeling of S-phase cells that is quantitated in Panel D and is increased significantly under SC culture conditions. By FACS analysis (Panel E), the uniform distribution of BrdU-positive cells across early-, mid- or late-S-phase shows that the BrdU-positive cells are indeed undergoing replicative DNA synthesis under SC culture conditions (21). Panel F demonstrates the decrease in BrdU-positive S-phase cells that accompanies the progression from log-phase growth in subconfluent (SC) culture to quiescence at postconfluent (PC) Day 5. Similar results were observed in the cultured mouse AEC cells MLE-12 (data not shown).

Figure 2 shows reductions in ACE-2 immunoreactive protein (Panel A), enzymatic activity (Panel B) and ACE-2 mRNA (Panel C) in either human A549 cells or mouse MLE-12 cells cultured under proliferating (SC) relative to quiescent (PC Day 5) conditions, both in the presence of growth factors. For each cell type, the enzymatic activity detected by fluorogenic peptide substrate (Panel B, see Methods) was essentially eliminated by the addition of peptide DX600 (DX), a competitive inhibitor of ACE-2 (23); these data demonstrate specificity of the activity assay when performed as described here. In Panel C, the mRNA for ACE-2 decreased to a degree similar to that observed for ACE-2 immunoreactive protein or enzymatic activity.

In a different experimental approach, A549 cells cultured to postconfluent quiescent conditions (in the presence of serum) were subjected to experimental wounding (the *in vitro* "scratch" model) to induce cell proliferation immediately adjacent to the scratch. Figure 3 shows postconfluent A549 cells immunolabeled for BrdU (Panels A & B) or ACE-2 (Panels C & D) in a region immediately adjacent to a scratch (at the top of each panel) as well as further away (bottom of each panel). In Panel A, cells at the edge of a scratch showed an increased BrdU labeling index relative to cells distal to the scratch. Panels C & D revealed a reduction in ACE-2 immunoreactivity in the proliferating cells immediately along the scratch edge (white arrows, Panel C), which are clearly visible in a phase contrast image of the same microscopic field (Panel D, black arrows).

To determine if this inverse relationship between ACE-2 and epithelial cell proliferation might be detected *in vivo* in response to growth factor–induced proliferation of AECs, C57BL6 mice were instilled intratracheally with keratinocyte growth factor (KGF), a known epithelial-specific mitogen active on alveolar epithelial cells (24,38). Figure 4 shows immunolabeling for ACE-2 (left panels) and BrdU (right panels), each performed on adjacent serial sections to insure colocalization within the same microenvironment. In normal mice (SHAM-instilled), ACE-2 immunolabeling was robust in epithelial cells within the alveolar corners (Panel A, brown), but BrdU immunolabeling in the same microenvironment was scant (B). In contrast, KGF-instilled mice examined two days after intratracheal instillation displayed reduced ACE-2 immunolabeling (C) in the same microenvironment where BrdU labeling was robust (D). Panel E shows the return of robust ACE-2 immunolabeling at two weeks after KGF instillation, a time at which KGF-induced AEC proliferation has subsided (24). Panel F documents a significant reduction in total lung tissue ACE-2 enzyme activity 2 days after KGF instillation.

To determine if this inverse relationship between ACE-2 and epithelial cell proliferation might be detected in the intact human lung, biopsy specimens obtained from patients with Idiopathic Pulmonary Fibrosis (IPF) or normal human lung were subjected to immunohistochemistry (IHC) for ACE-2, proliferating cell nuclear antigen (PCNA) and a specific immunologic marker of alveolar epithelial cells (monoclonal antibody MNF-116, see ref. 24). Figure 5 reveals that in normal human lung, immunoreactive ACE-2 was readily detected in epithelial cells within the alveolar corners (Panel A, brown), the normal location of type II pneumocytes. IHC for PCNA performed on a serial section of the same microenvironment revealed no proliferating epithelial cells (Panel B), consistent with the documented quiescence of type II pneumocytes in the normal, uninjured lung (24,19). In contrast, IHC for ACE-2 performed on a lung biopsy obtained from an IPF patient (Panel C) revealed essentially no ACE-2 immunoreactivity in the alveolar epithelium of a microenvironment in which the epithelium was heavily labeled with PCNA (Panel D, arrowheads), as detected in an adjacent serial section. Panel E depicts IHC for monoclonal antibody MNF-116 (brown) in a third adjacent serial section, to reveal that the epithelial layer was indeed being assessed by both the ACE-2 and PCNA antibodies. ACE-2-negative bronchial epithelia also were observed in IPF lung tissues (not shown).

In Figure 6, the culture system of subconfluent versus postconfluent human AEC cells was used to begin determining the mechanisms that might regulate ACE-2 expression as alveolar epithelial cells transition from subconfluent, proliferating cells to quiescent, postconfluent cells. Panel A shows that human A549 cells in subconfluent (SC) proliferating cultures (with relatively little ACE-2) gradually accumulate more immunoreactive ACE-2 with each day in postconfluent culture (PC1-5). With increasing time in postconfluent culture, cell proliferation (assessed by

BrdU labeling) gradually decreased to the 5-day postconfluent value shown in Figure 1B (BrdU time course not shown). Figure 6B shows that the transcription inhibitor actinomycin D, if added to the culture medium on either postconfluence day 4 (Act4) or postconfluence day 1 (Act1), could partially or completely block, respectively, the accumulation of immunoreactive ACE-2 protein that would otherwise occur by day 5 postconfluence. Panel C shows the SP600125, an inhibitor of c-Jun N-Terminal Kinase, could inhibit the accumulation of ACE-2 in A549 cells if added to culture medium on the first (JNKi-1) of five days in postconfluent culture (PC). In contrast, inhibitors of ERKs or p38-mediated signaling had no inhibitory effect on ACE-2 accumulation. These data suggest that the increase in ACE-2 that occurs as AECs transition from proliferating to quiescent cultures is regulated by a transcriptional mechanism mediated by JNK.

DISCUSSION

To our knowledge, this is the first report of regulation of ACE-2 expression as a function of cell cycle in any cell type or organ. In general, the control of ACE-2 expression is poorly understood in any system. In cardiac myocytes and fibroblasts, ACE-2 mRNA and protein is downregulated by angiotensin II or endothelin-1 (ET-1) and upregulated by the ANG receptor AT1 blocker losartan (25). The effects of either ANGII or ET-1 were prevented by inhibitors of mitogen-activated protein kinase (MAP kinase)-1, suggesting that the effects of these peptides might by mediated by extracellular signal-regulated (ERK) kinases. Angiotensin 1-7 (ANG1-7), one of the products of ACE-2 degradation of ANGII, also inhibited the decrease in ACE-2 mRNA in response to either ANGII or ET-1 through the ANG1-7 receptor *mas* (ibid).

In the mouse lung, ACE-2 has been shown to be developmentally regulated with mRNA highest at day 18.5 embryonically and to be expressed primarily in bronchiolar and alveolar epithelial cells (26). In the human lung, airway epithelial cells are one of the first sites of contact by the SARS coronavirus during lung infection; moreover, ACE-2 has been shown to be the site to which the SARS virus binds to initiate tissue infection (27). In studies of cultured human airway epithelial cells, shedding of the ACE-2 ectodomain is believed an important determinant of the extent and outcome of SARS infection (28). Related *in vitro* investigations have shown that shedding of the ACE-2 ectodomain is upregulated by phorbol esters and furthermore, is dependent on the binding of calmodulin to a specific binding domain in the cytoplasmic tail of ACE-2 (29). Although shedding of ACE-2 is believed to be important in SARS infection, the impact of either of these mechanistic determinants of ACE-2 ectodomain shedding, if any, on the physiological roles of pulmonary ACE-2 in the absence of SARS infection is currently unknown.

In cultured human pulmonary artery smooth muscle cells exposed to hypoxia *in vitro*, ACE-2 mRNA and protein were transiently upregulated in a manner dependent on the transcription factor HIF-1alpha (30). On the other hand, ACE-2 was downregulated in these cells by ANGII in a manner inhibitable by antagonists of AT1 receptor but not by receptor AT2 antagonists (ibid). Beyond these two works, little is known about the factors that regulate ACE-2 gene expression in lung cells. Although the works mentioned above suggest that ACE-2 levels in AECs might be responsive to changes in the steady state levels of ANGII or ANG1-7 (i.e. feedback loop) independent of cell proliferation, the addition of the ACE-2 inhibitor DX600 (5) during the progression from subconfluent to 5-day postconfluent cultures (as in Figure 6) had no apparent effect on the accumulation of ACE-2 (data not shown).

The data reported herein strongly support the hypothesis that ACE-2 expression in alveolar epithelial cells is regulated in a cell cycle-dependent manner, since ACE-2 mRNA, protein and enzymatic activity were all reduced in proliferating AECs relative to quiescent cells in postconfluent culture. Although the fluorogenic peptide substrate used here and elsewhere to measure ACE-2 is known to also function as a substrate for ACE-1, ICE (interleukin-1beta converting enzyme) and other peptidases (4), the elimination of ACE-2 activity by the addition of the competitive ACE-2 inhibitor peptide DX600 (Figure 2) lends support to our contention that the ACE-2 assay conditions used here yield measurements that are specific for ACE-2.

Similarly, the findings of reduced or absent ACE-2 immunoreactivity in A549 cells immediately adjacent to an *in vitro* wound (Figure 4) or within regions of fibrotic human lung with robust epithelial cell proliferation (Figure 5) argue against the contribution of cell culture artifacts to the substantial differences in ACE-2 expression observed in proliferating versus postconfluent AEC cell cultures. On this basis, it is hypothesized that the cell culture model of

proliferating versus postconfluent AEC cell lines described herein offers a viable experimental system with which to begin exploring the molecular mechanisms underlying the regulation of ACE-2 expression in a cell cycle-dependent manner. Our initial study of the mechanisms that underlie the upregulation of ACE-2 as cultured AECs enter quiescence (Figure 6) are consistent with the working hypothesis that ACE-2 gene transcription is increased by exit from the cell cycle through a JNK-mediated mechanism. Attempts to identify transcription factors and JNK-dependent signaling pathways active in this process are currently underway.

The potential physiological significance of such a cell cycle-dependent regulatory scheme for ACE-2 is currently unknown, but might be rationalized in the context of current thinking about the alveolar epithelium in human lung fibrosis. The classical observations of "hyperplastic" or "cuboidal" alveolar epithelia in fibrotic human lung are consistent with the long-held view that ongoing injury to the epithelium stimulates an attempt to repair epithelial damage through type II pneumocyte proliferation (18,19,31). Although myofibroblast foci underlying the abnormal epithelium in IPF are thought to influence epithelial cell survival (3,13), downregulation of ACE-2 in IPF lung biopsies studied here did not appear to be related spacially to the presence or absence of myofibroblast foci (data not shown). The failure of the epithelium to completely repair and replace the normal type II and type I cell populations, which was once thought to be primarily a result of disregulated proliferation or differentiation (32), is now known to be complicated by the consistent observation of epithelial apoptosis in the same microenvironment as AEC proliferation (3,33,34).

These two observation, although seemingly paradoxical, make sense when considered in the light of current knowledge regarding the signaling of cell division and cell death; in the control of either cell proliferation or apoptosis, cell cycle progression is required for both initial

signaling and execution (35). Moreover, recent studies demonstrated a critical role for the angiotensin system and in particular, ACE-2, its product ANG1-7 and JNK, in modulating the apoptotic response of AECs (5). Indeed, both human lung myofibroblasts and apoptotic alveolar epithelial cells have been shown to synthesize and secrete ANGII *in vitro* (9,10,13) and to express ANG peptides in the fibrotic human lung (3). Given the findings that ACE-2 is downregulated by ANGII in a manner inhibitable by ANG1-7 in cardiac myocytes and fibroblasts (25), it will be of great interest to examine the possibility that these same ANG peptides might play a regulatory role in the downregulation of ACE-2 gene expression in a cell cycle-dependent manner in the alveolar epithelium in human lung fibrosis. In that regard, several authors have performed retrospective analyses of the incidental use of ACE inhibitors in patients with IPF and reported no beneficial effect (36). However, as discussed recently by Budinger (37), the conclusion that these studies argue against a profibrotic role for ANGII in human lung fibrosis fails to acknowledge the demonstrated antifibrotic roles of the ACE-2 product ANG1-7 (5,16), which would be reduced by ACE inhibitor administration. For these reasons, angiotensin receptor blockers, but not ACE inhibitors, are currently of high interest in ongoing clinical trials designed for IPF patients (38).

ACKNOWLEDGEMENTS

This work was supported by PHS HL-45136 and by American Heart Association Grant-In-Aid 0950045G (B.D.U), and by grants from IDIBELL, España (M.M.M.)

REFERENCES

1. Li X, H Rayford and BD Uhal. Essential roles for angiotensin receptor AT1a in bleomycin-induced apoptosis and lung fibrosis in mice. *Am J Pathol* 2003;163(6):2523-2530.

2. Li X, J Zhuang, H Rayford, H Zhang, R Shu and BD Uhal. Attenuation of bleomycin-induced pulmonary fibrosis by intratracheal administration of antisense oligonucleotides against angiotensinogen mRNA. *Curr Pharm Design* 2007;13:1257-1268.

3. Li X, M Molina-Molina, A Abdul-Hafez, J Ramirez, A Serrano-Mollar, A Xaubet and BD Uhal. Extravascular sources of lung angiotensin peptide synthesis in idiopathic pulmonary fibrosis. *Am J Physiol Lung Cell Mol Physiol* 2006;291(5):L887-895.

4. Li X, Molina-Molina M, Abdul-Hafez A, Xaubet A and Uhal BD. Angiotensin converting enzyme-2 is protective but downregulated in human and experimental lung fibrosis. *Am J Physiol Lung Cell Mol Physiol* 2008;295(1):L178-L185.

5. Uhal BD, Li X, Xue A, Gao X, and Abdul-Hafez A. Regulation Of Alveolar Epithelial Cell Survival By The ACE-2/Angiotensin1-7/Mas Axis. *Am J Physiol Lung Cell Mol Physiol* 2011;301:L269-L274.

6. Marshall RP, McAnulty RJ, Laurent GJ. Angiotensin II is mitogenic for human lung fibroblasts via activation of the type 1 receptor. *Am J Respir Crit Care Med* 2000 Jun;161(6):1999-2004.

7. Königshoff M, Wilhelm A, Jahn A, Sedding D, Amarie OV, Eul B, Seeger W, Fink L, Günther A, Eickelberg O, Rose F. The angiotensin II receptor 2 is expressed and mediates angiotensin II

signaling in lung fibrosis. *Am J Respir Cell Mol Biol* 2007 Dec;37(6):640-50.

8. Marshall RP, Gohlke P, Chambers RC, Howell DC, Bottoms SE, Unger T, McAnulty RJ, Laurent GJ. Angiotensin II and the fibroproliferative response to acute lung injury. *Am J Physiol Lung Cell Mol Physiol* 2004 Jan;286(1):L156-164.

9. Wang, R., A. Zagariya, E. Ang, O. Ibarra-Sunga and B.D. Uhal. Fas-induced apoptosis of alveolar epithelial cells requires angiotensin II generation and receptor interaction. *Am J Physiol Lung Cell Mol Physiol* 1999;277:L1245-L1250.

10. Wang, R., G. Alam, A. Zagariya, C. Gidea, H. Pinillos, O. Lalude, G. Choudhary and B.D. Uhal. Apoptosis of lung epithelial cells in response to TNF-alpha requires angiotensin II generation de novo. *J Cell Physiol* 2000;185(2):253-259.

11. Li, X, H Zhang, V Soledad-Conrad, J Zhuang and BD Uhal. Bleomycin-induced apoptosis of alveolar epithelial cells requires angiotensin synthesis *de novo*. *Am J Physiol Lung Cell Mol Physiol* 2003;284(3):L501-L507.

12. Uhal BD, R Wang, J Laukka, J Zhuang, V Soledad-Conrad and G Filippatos. Inhibition of amiodarone-induced lung fibrosis but not alveolitis by angiotensin system antagonists. *Pharmacology and Toxicology* 2003; 92:81-87.

13. Uhal BD and M Molina-Molina. Angiotensin-TGF-β1 crosstalk in pulmonary fibrosis: autocrine mechanisms in myofibroblasts and macrophages. *Curr Pharm Design* 2007;13:1247-1256.

14. Abdul-Hafez A, R Shu and BD Uhal. JunD and HIF-1α mediate transcriptional activation of angiotensinogen by TGF-b1 in human lung fibroblasts. *FASEB J* 2009;23(6):1655-1662.

15. Otsuka M, Takahashi H, Shiratori M, Chiba H, Abe S. Reduction of bleomycin induced lung fibrosis by candesartan cilexetil, an angiotensin II type 1 receptor antagonist. *Thorax* 2004;59:31–38.

16. Shenoy V, Ferreira AJ, Qi Y, Fraga-Silva RA, Díez-Freire C, Dooies A, Jun JY, Sriramula S, Mariappan N, Pourang D, Venugopal CS, Francis J, Reudelhuber T, Santos RA, Patel JM, Raizada MK, Katovich MJ. The ACE2/Ang-(1-7)/Mas Axis Confers Cardiopulmonary Protection against Lung Fibrosis and Pulmonary Hypertension. *Am J Respir Crit Care Med* 2010;182:1065-1072.

17. Witschi, H. Responses of the lung to toxic injury. *Environ Health Perspect* 1990; 85:5-13.

18. Selman M. Pulmonary fibrosis: Human and experimental disease. In: Rojkind M ed. Connective Tissue in Health and Disease. CRC Press Inc. Boca Raton FL, 1990; 123-188.

19. Uhal, B.D. Cell cycle kinetics in the alveolar epithelium (Invited Review). *Am J Physiol Lung Cell Mol Physiol* 1997; 272:L1031-L1045.

20. Raghu G, Collard HR, Egan JJ, Martinez FJ, Behr J, Brown KK, et al. An official ATS/ERS/JRS/ALAT statement: idiopathic pulmonary fibrosis: evidence-based guidelines for diagnosis and management. *Am J Respir Crit Care Med*. 2011;183(6):788-824.

21. Uhal, B.D., Flowers, K.M. and Rannels, D.E. Type II pneumocyte proliferation in vitro: problems and future directions. (Invited Review) *Am J Physiol Lung Cell Mol Physiol Suppl* 1991;261:110-117.

22. Uhal, B.D. and Rannels, D.E. DNA distribution analysis of type II pneumocytes by laser flow cytometry: technical considerations. *Am J Physiol Lung Cell Mol Physiol* 1991;261:L296-L306.

23. Huang L, Sexton DJ, Skogerson K, Devlin M, Smith R, Sanyal I, Parry T, Kent R, Enright J, Wu QL, Conley G, DeOliveira D, Morganelli L, Ducar M, Wescott CR, Ladner RC. Novel peptide inhibitors of angiotensin-converting enzyme 2. *J Biol Chem* 2003; 278:15532-15540.

24. Fehrenbach H. Alveolar epithelial type II cell: defender of the alveolus revisited. *Respir Res* 2001;2(1):33-46.

25. Gallagher PE, Ferrario CM, Tallant EA. Regulation of ACE2 in cardiac myocytes and fibroblasts. *Am J Physiol* 2008;295(6):H2373-9.

26. Weiner RS, Cui YX, HindsA, Ramirez MI, Williams MC. Angiotensin conerting enzyme 2 is primarily epithelial and is developmentally regulated in the mouse lung. *J Cell Biochem* 2007;101:1278-1291.

27. Li W, Moore MJ, Vasilieva N, Sui J, Wong SK, Berne MA, Somasundaran M, Sullivan JL, Luzuriaga K, Greenough TC, Choe H, Farzan M. Angiotensin-converting enzyme 2 is a functional receptor for the SARS coronavirus. *Nature* 2003;426:450-454.

28. Jia HP, Look DC, Tan P, Shi L, Hickey M, Gakhar L, Chappell MC, Wohlford-Lenane C, McCray PB. Ectodomain shedding of angiotensin converting enzyme 2 in human airway epithelia. *Am J Physiol Lung Cell Mol Physiol* 2009;297(1):L84-96.

29. Lai ZW, Lew RA, Yarski MA, Mu FT, Andrews RK, Smith AI. The identification of a calmodulin-binding domain within the cytoplasmic tail of angiotensin-converting enzyme-2. *Endocrinology*. 2009;150(5):2376-81.

30. Ruifeng Zhang, Yingli Wu, Meng Zhao, Chuanxu Liu, Lin Zhou, Shaoming Shen, Shihua Liao, Kun Yang, Qingyun Li and Huanying Wan. Meng Zhao, Chuanxu Liu, Lin Zhou, Shaoming Shen, Role of HIF-1α in the regulation ACE and ACE2 expression in hypoxic human pulmonary artery smooth muscle cells. *Am J Physiol Lung Cell Mol Physiol* 2009;297:L631-L640.

31. Haschek, W.M. and H.P. Witschi. Pulmonary fibrosis: a possible mechanism. *Toxicol Appl Pharmacol* 1979;51:75-487.

32. Simon, R.H. Alveolar epithelial cells in pulmonary fibrosis. In: Pulmonary Fibrosis, S.H. Phan and R.S. Thrall, Eds., In: Lung Biology in Health and Disease, C. Lenfant, Ed., Vol. 80, p. 511-540, 1995.

33. Uhal, B.D., Joshi, I, Ramos, C., Pardo, A. and M. Selman. Alveolar epithelial cell death adjacent to underlying myofibroblasts in advanced fibrotic human lung. *Am J Physiol Lung Cell Mol Physiol* 1998;275:L1192-L1199.

34. Plataki M, Koutsopoulos AV, Darivianaki K, Delides G, Siafakas NM, Bouros D. Expression of apoptotic and antiapoptotic markers in epithelial cells in idiopathic pulmonary fibrosis. *Chest* 2005;127:266–274.

35. Eastman, A. Apoptosis: A product of programmed and unprogrammed cell death. *Toxicol Appl Pharmacol* 1993;121:160-164.

36. Nadrous HF, Ryu JH, Douglas WW, Decker PA, Olson EJ. Impact of angiotensin-converting enzyme inhibitors and statins on survival in idiopathic pulmonary fibrosis. *Chest* 2004;126:438–446.

37. Budinger GR. Angiotensin II and pulmonary fibrosis, a new twist on an old story. *Am J Physiol Lung Cell Mol Physiol*. 2011;301:L267-268.

38. Datta A, Scotton C, Chambers R. Novel therapeutic approaches for pulmonary fibrosis. *British Journal of Pharmacology* 2011;163:141-172.

FIGURE LEGENDS

Figure 1. Manipulation of cell cycle status in cultured human lung epithelial cells. The human alveolar epithelial cell line A549 was cultured under subconfluent or postconfluent conditions, both in the presence of growth factors, as described in Materials and Methods. A: Phase contrast micrograph of A549 cells at postconfluent (PC) Day 2; note lack of binucleated or mitotic cells (compare to B). B: Phase contrast micrograph of subconfluent (SC) A549 cells; note binucleated cells undergoing cytokinesis. C: BrdU-FITC labeling of S-phase A549 cells under SC culture conditions. D: Percentage of BrdU-positive nuclei under the culture conditions PC versus SC. Bars are the mean + S.E.M of at least three cell cultures; * = $p<0.05$ versus PC by Student's t-test. E: Bivariate flow cytometric analysis of DNA distribution (x-axis) versus incorporated BrdU (y-axis) of subconfluent A549 cells; note uniform distribution of BrdU-positive cells across S-phase DNA content (21). F: Quantitation of decreasing BrdU labeling of A549 cells during the progression from subconfluence to Day5 postconfluence. Bars are the mean + S.E.M of at least three cell cultures; * = $p<0.01$ versus SC by ANOVA and Student-Newman-Keul's test. See text for details

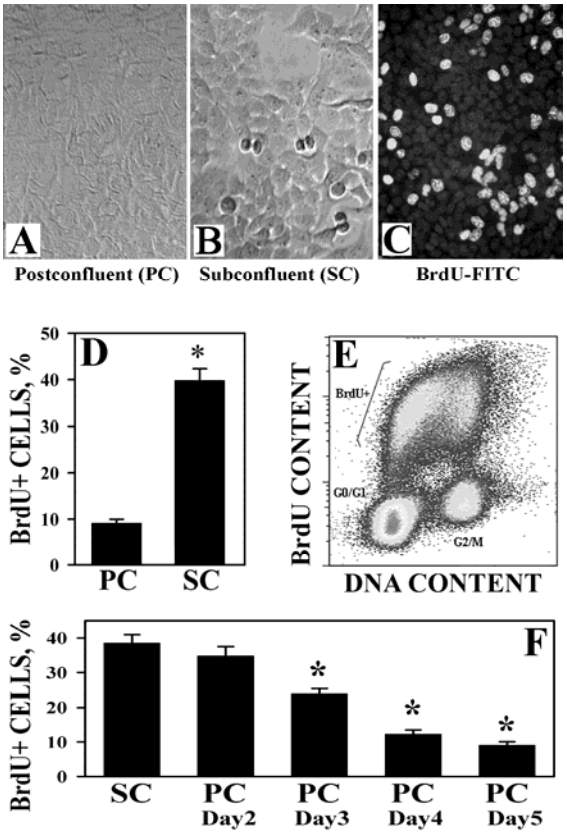

Figure 2. Downregulation of ACE-2 protein, enzymatic activity and mRNA with proliferation of human and mouse alveolar epithelial cells in culture. The human and mouse alveolar epithelial cell lines A549 or MLE-12, respectively, were cultured at postconfluent (PC) and subconfluent (SC) densities as described in Materials and Methods and were then harvested for western blotting (Panel A), ACE-2 enzyme assay (Panel B) or mRNA by RTPCR (Panel C). Panel A shows a representative example of three similar blots from three separate experiments. In Panel B, lysates from cells cultured under PC conditions were also assayed in the presence of DX600 (DX), a competitive inhibitor of ACE-2. Note essentially complete inhibition by peptide DX600 (1uM). Bars are the mean + S.E.M of at least three cell cultures; * = $p<0.05$ versus PC and ** = $p<0.01$ versus PC by ANOVA and Student-Newman Keul's post hoc test.

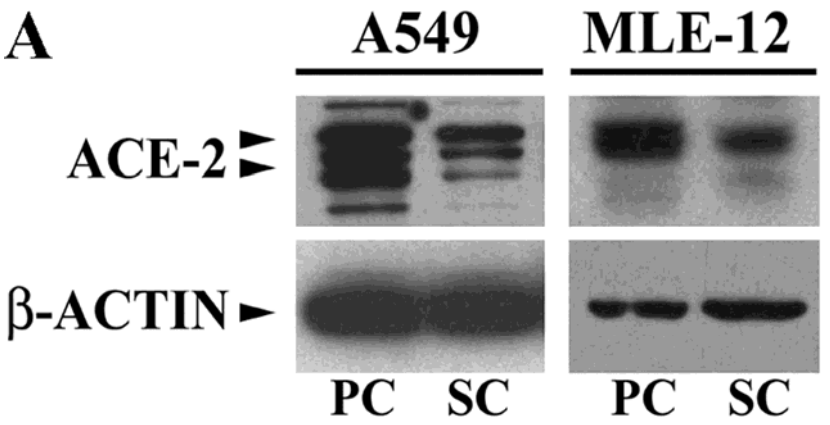
A
A549
MLE-12
ACE-2
β-ACTIN
PC
SC
PC
SC

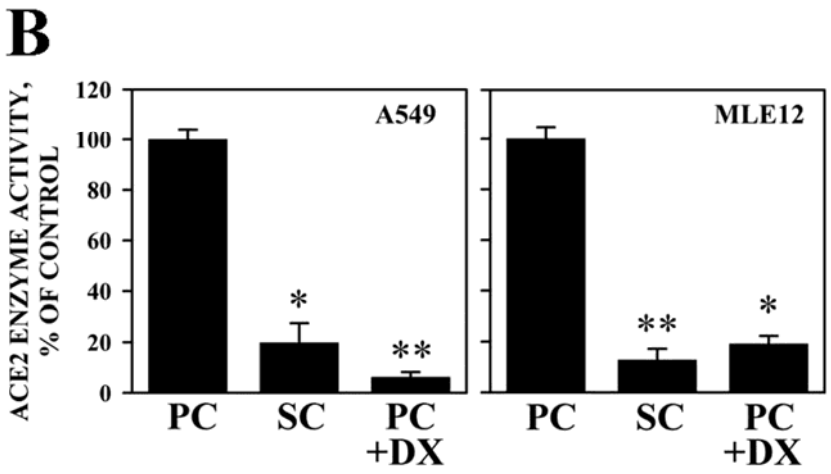
B
ACE2 ENZYME ACTIVITY, % OF CONTROL
120
100
80
60
40
20
0
A549
MLE12
*
**
**
*
PC
SC
PC +DX
PC
SC
PC +DX

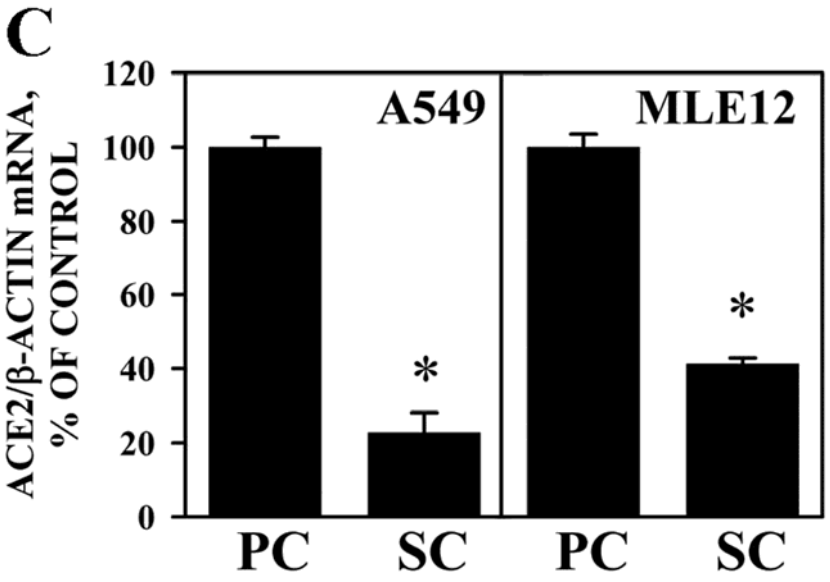
C
ACE2/β-ACTIN mRNA, % OF CONTROL
120
100
80
60
40
20
0
A549
MLE12
*
*
PC
SC
PC
SC

Figure 3. Downregulation of ACE-2 immunoreactivity in human alveolar epithelial cells repairing a wound *in vitro*. The human cell line A549 was cultured to postconfluent density and subjected to wounding of the monolayer by scratch followed by a short exposure to BrdU (see Material and Methods). Monolayers were then fixed and immunolabeled with antibodies against BrdU (A and B) or ACE-2 (C and D). In each pair, the left or right panels show immunolabeling (A&C) or phase contrast (B&D) images of the same 100X microscopic field. In all panels, the scratch is at the top. Note the area of cells immediately adjacent to the scatch (Panel D, black arrows) that are mostly negative for ACE-2 immunoreactivity (Panel C, white arrows). Note also the increased density of BrdU-positive nuclei immediately adjacent to the scratch (Panel A, upper quadrant) when compared to the density distal to the scratch (Panel A, lower quadrant). Quantitation of BrdU-positive nuclei and ACE-2-positive cells at the edge of the scratch versus at the center of the monolayer are indicated. Values are the mean + S.E.M of at least three cell cultures; both BrdU+ and ACE-2+ values are significant to $p<0.05$ by Student's t-test.

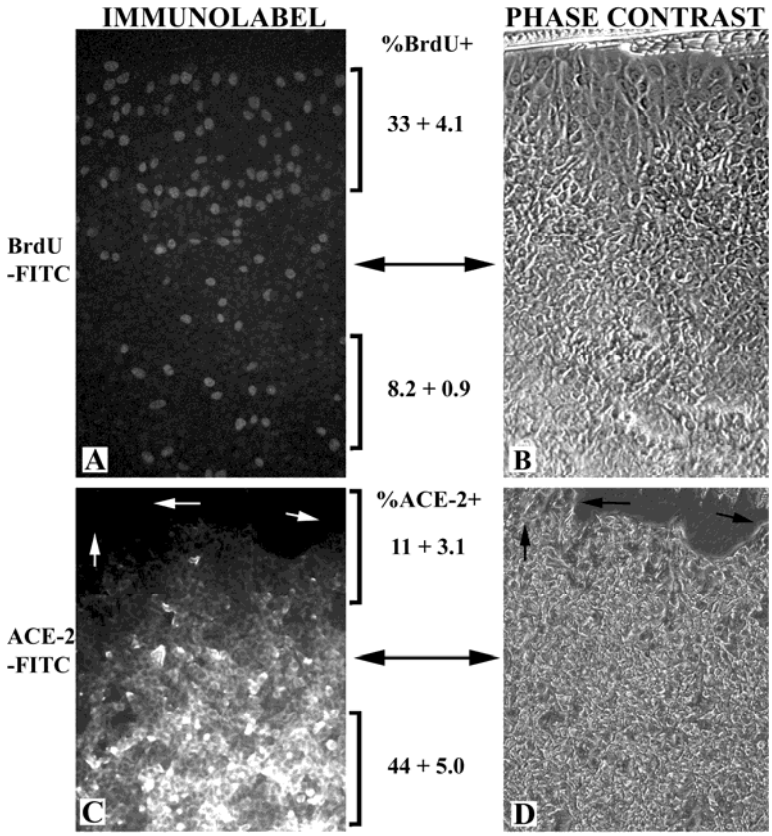

Figure 4. Downregulation of ACE-2 in proliferating epithelia of mouse lung instilled with keratinocyte growth factor (KGF) lung *in situ*. C57BL6 mice were administered purified recombinant KGF or vehicle (SHAM) intratracheally as described in Materials and Methods. One hour before sacrifice, animals were administered BrdU (50mg/kg i.p.) for identification of proliferating cells (21). Lung sections were immunolabeled with antibodies against ACE-2 (Panels A,C,E) or BrdU (B,D). Panel F: lungs were homogenized for ACE-2 enzyme assay; bars are the mean +/- S.E.M of n=4 each for SHAM and KGF Day 2. See Materials and Methods for details.

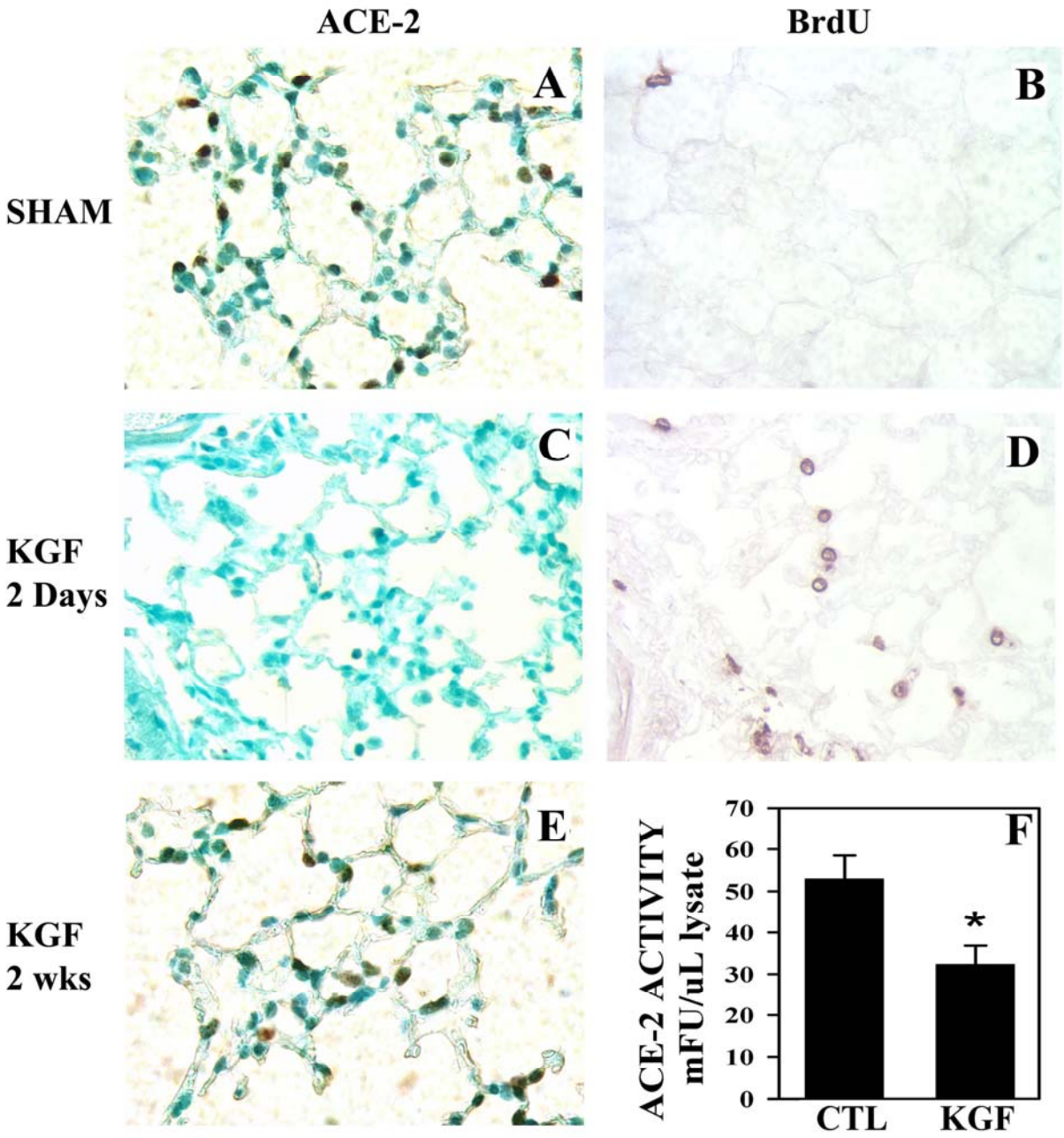

Figure 5. Downregulation of ACE-2 in proliferating epithelia of human IPF lung *in situ*. Paraffin sections of biopsy specimens of normal human lung (A,B) or IPF human lung (C,D,E) were subjected to immunohistochemistry for ACE-2, PCNA or MNF-116 as described in Materials and Methods. A: Heavy labeling of ACE-2 (brown) in alveolar corner cells within normal human

lung, magnification 400X; B: Negative labeling of PCNA (contrast with D) in the same microenvironment of a serial section adjacent to that analyzed in Panel A; C: Negative labeling for ACE-2 in epithelia of IPF human lung (contrast with A), magnification 400X; D: Heavy labeling of PCNA (arrowheads) in the same epithelia of IPF lung (a serial section adjacent to that in C); E: Positive labeling by antibody MNF-116 (brown) in another serial section (adjacent to that in D) identifies the epithelial layer studied in C and D. F: Low magnification view (100X) of the same region from which Panel A was derived; brown = ACE-2 positive cells. G: Low magnification view (100X) of the same region from which Panel C was derived. See Materials and Methods for details and descriptions of the patient populations.

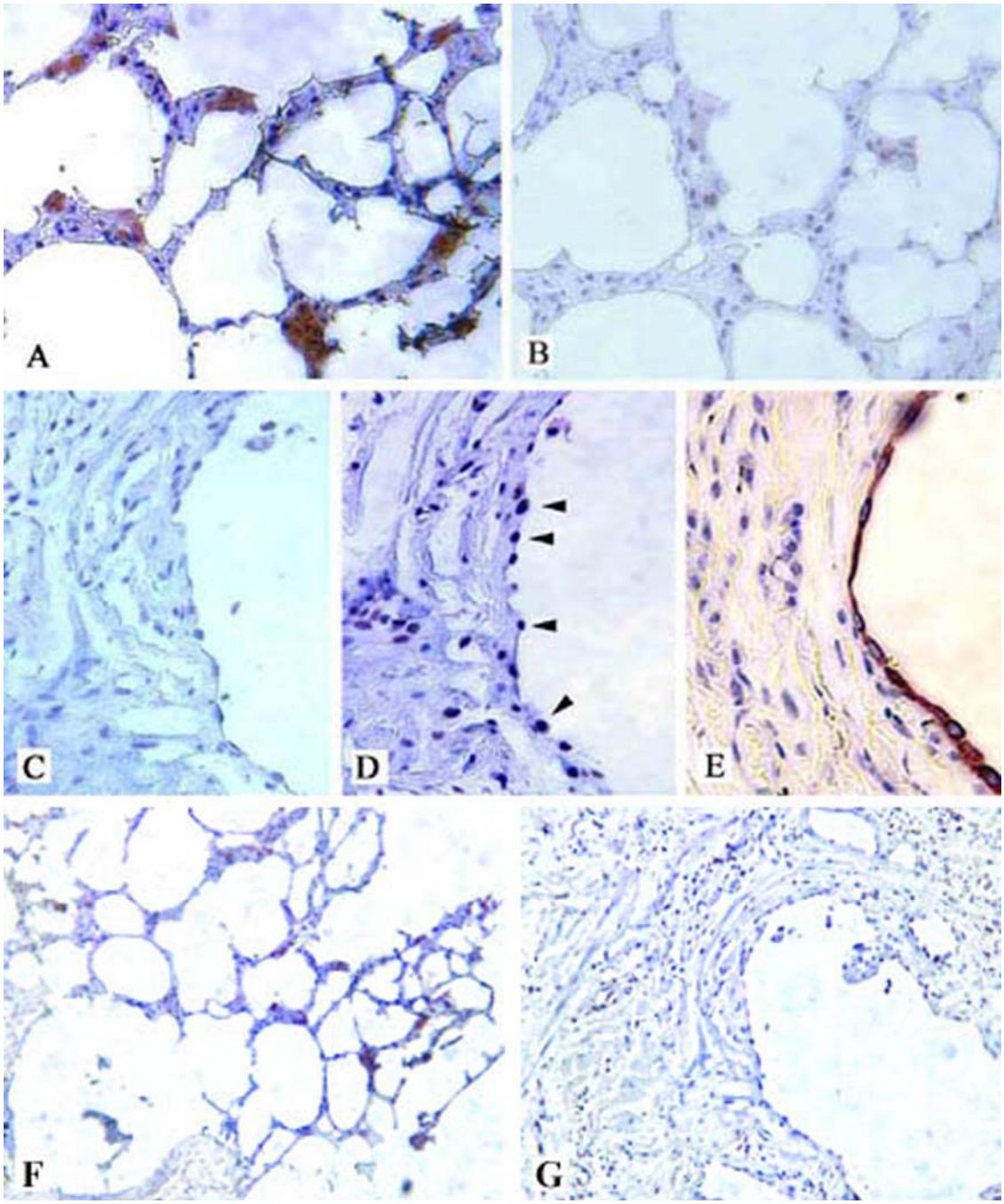

Figure 6. Evidence for JNK-mediated transcriptional control of ACE-2 upregulation in the epithelial transition from cell cycling to quiescence. The human cell line A549 was cultured at subconfuent density (SC) and monitored daily by western blotting during the transition to

postconfluent quiescence (PC), either in the presence or absence of actinomycin D (Act), vehicle DMSO (D) or inhibitors of JNK (JNKi), ERKs (ERKi) or p38 (p38i)- mediated signaling pathways. See Methods for details; all panels show a representative example of at least three similar blots from three separate experiments.

A: Increase in immunoreactive ACE-2 as a function of time (days) in postconfluent culture (PC) relative to subconfluenct (SC) cultures.

B: Blockage of ACE-2 upregulation over five days postconfluent culture (PC5) of A549 cells by the addition of actinomycinD (1ug/ml) on postconfluence day 4 (Act4) or postconfluence day 1 (Act1). Note similarity of ACE-2 expression under Act1 conditions to that observed in subconfluent culture (SC in Panel A).

C: Blockage of ACE-2 upregulation over five days postconfluent culture (PC) of A549 cells by the addition of SP600125 (10uM) on postconfluence day 1 (JNKi-1), but not by inhibitors of ERKs (PD98059, 10uM) or p38 (SB203580, 10uM) applied in the same manner. D = vehicle alone (0.1% DMSO in F12 media).

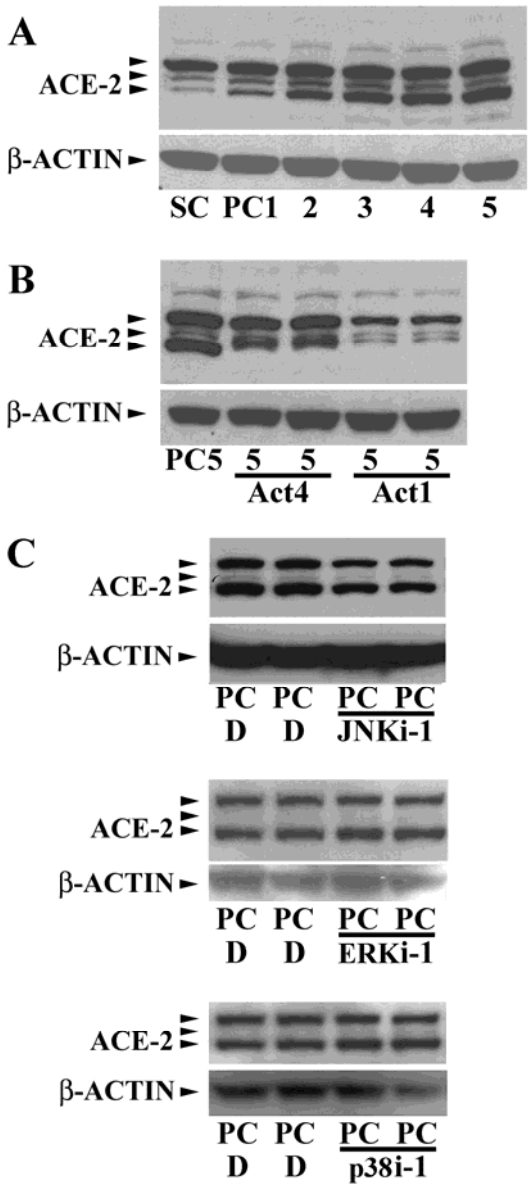
A
ACE-2
β-ACTIN
SC PC1 2 3 4 5
B
ACE-2
β-ACTIN
PC5 5 5 5 5
Act4 Act1
C
ACE-2
β-ACTIN
PC PC PC PC
D D JNKi-1
ACE-2
β-ACTIN
PC PC PC PC
D D ERKi-1
ACE-2
β-ACTIN
PC PC PC PC
D D p38i-1